Journal of Molecular and Cellular Cardiology 180 (2023) 10–21

Contents lists available at ScienceDirect

Journal of Molecular and Cellular Cardiology

journal homepage: www.elsevier.com/locate/yjmcc

Reduced O-GlcNAcylation diminishes cardiomyocyte Ca^{2+} dependent facilitation and frequency dependent acceleration of relaxation

Andrew R. Ednie *, Chiagozie D. Paul-Onyia, Eric S. Bennett

Department of Neuroscience, Cell Biology & Physiology, Boonshoft School of Medicine and College of Science and Mathematics, Wright State University, Dayton, OH, USA

ARTICLE INFO

Keywords:
Voltage-gated Ca^{2+} channel
Ca^{2+}-induced Ca^{2+} release
O-GlcNAcylation
CaMKII

ABSTRACT

Ca^{2+} dependent facilitation (CDF) and frequency dependent acceleration of relaxation (FDAR) are regulatory mechanisms that potentiate cardiomyocyte Ca^{2+} channel function and increase the rate of Ca^{2+} sequestration following a Ca^{2+}-release event, respectively, when depolarization frequency increases. CDF and FDAR likely evolved to maintain EC coupling at increased heart rates. Ca^{2+}/calmodulin-dependent kinase II (CaMKII) was shown to be indispensable to both; however, the mechanisms remain to be completely elucidated. CaMKII activity can be modulated by post-translational modifications but if and how these modifications impact CDF and FDAR is unknown. Intracellular O-linked glycosylation (O-GlcNAcylation) is a post-translational modification that acts as a signaling molecule and metabolic sensor. In hyperglycemic conditions, CaMKII was shown to be O-GlcNAcylated resulting in pathologic activity. Here we sought to investigate whether O-GlcNAcylation impacts CDF and FDAR through modulation of CaMKII activity in a pseudo-physiologic setting. Using voltage-clamp and Ca^{2+} photometry we show that cardiomyocyte CDF and FDAR are significantly diminished in conditions of reduced O-GlcNAcylation. Immunoblot showed that CaMKIIδ and calmodulin expression are increased but the autophosphorylation of CaMKIIδ and the muscle cell-specific CaMKIIβ isoform are reduced by 75% or more when O-GlcNAcylation is inhibited. We also show that the enzyme responsible for O-GlcNAcylation (OGT) can likely be localized in the dyad space and/or at the cardiac sarcoplasmic reticulum and is precipitated by calmodulin in a Ca^{2+} dependent manner. These findings will have important implications for our understanding of how CaMKII and OGT interact to impact cardiomyocyte EC coupling in normal physiologic settings as well as in disease states where CaMKII and OGT may be aberrantly regulated.

1. Introduction

Cardiomyocyte L-type voltage gated Ca^{2+} channels (Ca_vs) control the influx of extracellular Ca^{2+} (I_{Ca}) and are therefore the main trigger for excitation-contraction (EC) coupling in the heart [1]. In addition to their basal properties, Ca_vs can be dynamically regulated so that the heart can respond to changes in physiologic demand [2,3]. Ca^{2+} dependent facilitation (CDF) is a positive feedback regulatory mechanism that results in increased Ca^{2+} entry through Ca_vs and/or slower Ca_v inactivation when depolarization frequency increases [3]. CDF likely evolved as a response to the negative feedback process of Ca^{2+}-dependent inactivation (CDI) that accelerates Ca_v inactivation when $[Ca]_i$ rises to protect the cell from Ca^{2+} overload [4]. Thus, the physiologic role of CDF is likely to maintain EC coupling when heart rate increases. Working in concert with CDF is frequency dependent acceleration of relaxation (FDAR) whereby the sequestration of $[Ca]_i$ following a Ca^{2+} release event is accelerated when stimulation rate increases [5,6].

The overwhelming evidence indicates that CDF and FDAR are attributed to the activity of the Ca^{2+} and calmodulin dependent kinase, CaMKII. This was largely gleaned from studies showing abolishment and/or significant reductions in CDF and FDAR following pharmacologic inhibition of CaMKII [6–11]. Our current understanding of how CaMKII mediates CDF is by direct phosphorylation of Ca_vs likely at Ser1512(1517) and/or Ser1570 of the α subunit [12,13]. This alters the gating properties of individual Ca_vs resulting in longer and more frequent openings. Despite these findings, much remains unknown. For example, in a mouse model where both putative CDF-related targets of CaMKII (Ser1512 and Ser1570 of mouse Ca_vα) were mutated to Ala, CDF

* Corresponding author at: Department of Neuroscience, Cell Biology & Physiology - Boonshoft School of Medicine, Wright State University, 143 Biological Sciences II, 3640 Colonel Glenn Hwy, Dayton, OH 45435, USA.
E-mail address: andrew.ednie@wright.edu (A.R. Ednie).

https://doi.org/10.1016/j.yjmcc.2023.04.007
Received 4 August 2022; Received in revised form 12 April 2023; Accepted 19 April 2023
Available online 28 April 2023

was reduced but not abolished [12]. Additionally, while there are several CaMKII isoforms found in the heart, CaMKIIδ is the predominant isoform [14,15]; however, genetic ablation of CaMKIIδ also reduced but did not abolish CDF [16]. These results raise the questions that other mechanisms and multiple CaMKII isoforms may contribute to CDF and FDAR. Despite these discrepancies, in a mouse model where CaMKII inhibition was targeted to the sarcoplasmic reticulum (SR) of cardiomyocytes, CDF was abolished and FDAR was markedly reduced [5] indicating that localization to the SR and/or the dyad space is critical to regulating CDF and FDAR. In addition to these unresolved issues regarding the mechanisms by which CaMKII contributes to CDF and FDAR and what isoforms may be responsible, it is also largely unknown whether other signaling pathways that can impact CaMKII activity [17] may also contribute to CDF and FDAR.

CaMKII can be post-translationally modified by oxidation, S-nitrosylation, autophosphorylation and, discovered only recently, intracellular O-linked glycosylation (O-GlcNAcylation) [18,19]. These modifications typically cause CaMKII to be trapped in an autonomous state that result in increased activity [18,19]. If and how these modifications impact CDF and FDAR in vivo is not known. O-GlcNAcylation is characterized by the dynamic shuttling of *N*-acetylglucosamines (GlcNAc) to intracellular serine and threonine residues, akin to phosphorylation [20]. O-GlcNAc transferase (OGT) and O-GlcNAcase (OGA) are the only two enzymes known to add (OGT) or remove (OGA) O-GlcNAc residues [21]. In addition to functioning as a signaling molecule, OGT is considered a nutrient-sensor because production of UDP-GlcNAc, the substrate of OGT, requires processing of glucose or other metabolites through the hexosamine biosynthesis pathway [22]. This metabolite-sensing property of OGT is likely why aberrant O-GlcNAcylation is implicated in diseases like diabetes mellitus and heart failure, where metabolic substrate utilization is altered [23–25]. While not as well understood as phosphorylation, the complexity and scope of O-GlcNAc signaling in the heart is emerging at an accelerating rate [26]. By creating a cardiomyocyte-specific *OGT*-null mouse strain (OGTKO), we recently showed for the first time that OGT is a critical and direct regulator of multiple aspects of Ca_v function [27]. Cardiomyocytes from OGTKO mice showed marked reductions in I_{Ca} density and post-transcriptional expression, depolarizing shifts in voltage-dependent gating and increased efficacy of adrenergic stimulation [27]. Heart and cardiomyocyte EC coupling were also consistently reduced in the OGTKO [27]. While these findings were a critical first step in uncovering a new role for O-GlcNAc signaling in the heart, they are likely only a primer given the extensive cross-talk O-GlcNAcylation displays with other signaling molecules that regulate Ca_vs and cardiomyocyte EC coupling such as CaMKII.

Work by the Bers group indicated that CaMKII O-GlcNAcylation occurs in conditions of hyperglycemia and that the resulting O-GlcNAcylated CaMKII demonstrates increased and, in most cases, pathologic activity [28–31]. This activity is like the activity incurred by increased CaMKII autophosphorylation. Their data also suggest that these two post-translational modifications occur independently of each other [28,29]. This spurred us to question whether OGT and CaMKII demonstrate a broader interaction that could be observed in a pseudo-physiologic setting. Thus, in the present study, we tested whether OGT inhibition could impact CDF and FDAR in the absence of any other pathophysiologic stimuli such as hyperglycemia. Our data indicate that in conditions of chronic and acute OGT inhibition, CDF and FDAR are both significantly depressed. We also observed that chronic reductions in O-GlcNAcylation result in increased CaMKIIδ and calmodulin expression but nearly abolished CaMKII autophosphorylation. The data indicate that the relationship between OGT and CaMKII is more complex than previously thought and can occur in non-hyperglycemic conditions. These findings will have important ramifications for our understanding of how CaMKII and OGT interact to impact cardiomyocyte EC coupling in normal physiologic settings as well as in other disease states where CaMKII and OGT may be aberrantly regulated.

2. Methods

2.1. Ethical approval

Animals were handled in accordance with the NIH Guide for the Care and Use of Laboratory Animals. All protocols involving animals were approved by the Wright State University Institutional Animal Care and Use Committee (AUP 1163). Mice were euthanized, under deep anesthesia (5% isoflurane), by thoracotomy and excision of the heart to obtain samples for the biochemical and functional studies.

2.2. Animal use

The cardiomyocyte-specific *OGT*-null OGTKO strain was created as previously described [27]. *OGT* is X-linked and others have shown that induced male OGTKO mice demonstrate low mosaicism [32] while female mice possess a much greater risk for heterogeneity likely due to incomplete X-linked inactivation [33]. Low levels of mosaicism are critical when performing single-cell experiments; therefore, 12–16-week-old male mice were used in all experiments. However, to ensure sex differences do not exist with regards to the effects of cardiomyocyte *OGT* deletion on Ca_v function, a study on female OGTKO mice was performed [supplemental fig. 1 (SF1)] and indicated similar results on Ca_v activity as reported previously [27] and here (Fig. 1). To control for potential spurious effects of tamoxifen induction and α-MHC-MerCreMer expression [34,35], all control mice for the OGTKO strain were tamoxifen treated and α-MHC-MerCreMer positive but had a normal OGT gene. A two-week regiment of tamoxifen-containing chow (250mgs/kg; TD.130855; Envigo, Indianapolis, IN, USA) was used for induction. OGTKO and control animals were used 22–30 days post induction. C57BL6 wild-type mice were originally from Jackson Laboratories but the mice used in this study were from a colony maintained at the Wright State University Laboratory Animal Resources Department.

2.3. Cardiomyocyte isolation

Cardiomyocytes from the left ventricular (LV) wall were isolated using 0.6–1 mg/ml collagenase type II (CLS2; Worthington, Lakewood, NJ, USA) and 0.5 u/ml protease XIV (P5147; Sigma Aldrich, Saint Louis, MO, USA) via Langendorff perfusion as previously described [27,36,37]. Myocytes were stored in Hank's balanced salt solution buffered with 10 millimoles/l (mM) (4-(2-hydroxyethyl)-1-piperazineethanesulfonic acid (HEPES) K^+ salt and supplemented with 1× MEM amino acids (11,130,051 and 11,140,050; Thermo Fisher Scientific, Waltham, MA, USA) at room temperature. Myocytes were used 1–6 h following isolation.

2.4. Cellular electrophysiology

Ca_v activity was recorded at room temperature as previously described [27,36,38]. In brief, cardiomyocytes were added to a recording chamber and bathed in a solution consisting of the following in mM: 136 NaCl, 1 MgCl2, 1 CaCl2, 10 glucose, 10 HEPES, 4 CsCl, 0.02 tetrodotoxin (TTX); pH 7.4-NaOH. Cells were ruptured following seal formation and dialyzed (5 min) with an intracellular recording solution (in mM): 110 Cs^+ methane sulfonate, 30 CsCl, 10 HEPES, 1.0 $CaCl_2$, 2 $MgCl_2$, 5 Na_2ATP, 5 EGTA; pH 7.2-CsOH. To explore the effects of intracellular Ca^{2+} on CDF and recovery from inactivation and determine whether the effects differed in conditions of reduced O-GlcNAcylation, in a subset of experiments, Ca^{2+} was omitted and the EGTA concentration was raised to 10 mM in the intracellular recording solution. At 10 mM EGTA, a global increase in intracellular Ca^{2+} is prevented but because of the relatively slow onset of Ca^{2+} buffering by EGTA, an accumulation of Ca^{2+} at the mouth of the channel will still occur upon depolarization [3,5,9]. To specifically investigate the impact of Ca^{2+} release from the SR via ryanodine receptors on CDF and recovery from

inactivation, 2 μM ryanodine (1329; Tocris, Bristol, UK) was added to the extracellular recording solution and cells were incubated for a minimal of 30 min prior to patching.

Cells were voltage clamped at −50 mV and cell size was determined by integrating the capacitance of the cell following a 25 ms, 10 mV step in voltage. Series resistance and capacitance errors were compensated at 70%. Analog signals were low-pass filtered (5 kHz) then digitized (50 kHz) and voltage clamp protocols were written and executed using Clampex 10.7 (Molecular Devices, Sunnyvale, CA, USA). Leak currents were always fewer than 50 pA and were ignored. To record steady-state Ca_v activity, cells were clamped at −50 mV then depolarized by a series of voltage steps beginning at −40 mV and ending at 60 mV for 200 ms in 10 mV increments. The voltage steps were separated by 15 s. The maximum negative current at each test pulse was divided by capacitance for each cell and averaged to report the I_{Ca}–density/voltage relationships.

To record CDF, cells were clamped at −90 mV, depolarized to −40 mV for 50 ms to inactivate any voltage-gated Na^+ channels (Na_vs) not blocked by TTX, and depolarized to 10 mV for 200 ms. After reaching a steady-state, this was repeated 10 times at 0.5 Hz. CDF was determined by calculating the percent increase in current of pulses 2–10 versus the current from pulse 1. To compare the effects of CDF on Ca_v inactivation, the time required for the I_{Ca} to decay one exponential unit or to 37% of the peak ($T_{0.37}$) was calculated and compared between the pulse (P) 1 and P2 currents as done by others [11]. The percent change between P1 and P2 $T_{0.37}$ was then calculated.

Ca_v recovery from inactivation was recorded using a standard two-pulse protocol to a test potential of 10 mV from a holding potential of −90 mV. A 50 ms step to −40 mV to inactivate Na_vs preceded the 10 mV step. The rest intervals ranged from 50 to 3000 ms. Fractional current (I_2/I_1) from each two-pulse sweep was plotted as a function of rest interval and the curve was fit with a mono-exponential function to calculate the rate of recovery, which was reported as the time constant (Tau). The Tau values from each cell of a group were averaged to compare recovery rates but the figures indicate the mean I_2/I_1 values for all the cells in a group.

2.5. Ca^{2+} transients

Ca^{2+} transients were recorded at room temperature as previously described [27,36,37]. Briefly LV cardiomyocytes were loaded with 1 μM of the ester form of fura-8 (21-056; AAT Bioquest, Sunnyvale, CA, USA) for 20 min and the dye was allowed to de-esterify for 30 min. Fura-8 is a newer, red-shifted ratiometric Ca^{2+} dye that demonstrates better sensitivity and signal-to-noise than fura-2. Loaded myocytes were added to a recording chamber filled with Tyrode's solution (in mM: 136 NaCl, 4 KCl, 1 $CaCl_2$, 1 $MgCl_2$, 10 glucose, and 10 HEPES; pH 7.4-NaOH) and outfitted with platinum stimulation electrodes. Myocytes were allowed to settle, and cells were stimulated with 10 V at 0.5 and 3 Hz (MyoPacer; IonOptix, Westwood, MA, USA). Ca^{2+} signals were recorded ratiometrically by alternating the excitation wavelengths between 355 and 415 nm at 200 Hz using a monochromator, and emission was filtered (510/84 nm; Semrock, Rochester, NY, USA) and detected with a photometry system (PTI RatioMaster; Horiba Scientific, Edison, NJ, USA). Ca^{2+} transients were analyzed with IonWizard 7.4 (IonOptix, Westwood, MA, USA) and the decay portion of the last Ca^{2+} transient of the train at each stimulation frequency was fit with a mono-exponential function. The time constant of the exponential fit (Tau) was used as a measure of decay rate and the last transient of the train was analyzed to ensure that the rate of decay was not underestimated at the 3 Hz stimulation frequency.

2.6. Immunoblotting

Control and OGTKO ventricles were homogenized in HEPES buffered saline supplemented with 0.5% amidosulfobentaine, 1× Complete Ultra protease inhibitor cocktail (5-892-970-001; Roche, Mannheim, DE), 0.01 calpain inhibitors I and II (A2602 and A2603; Apex Bio, Houston, TX, USA), 0.001 thiamet G (13-237; Caymen Chemical, Ann Arbor, Michigan, USA) and 0.02% Na^+ azide. Gel electrophoresis and Western blotting using a bis-tris based buffer system was performed as previously described [27,36–38]. Immunodetection was carried out using the following commercially available antibodies: anti-CaMKIIδ and anti-calmodulin (A9196 and A4885 respectively; Abclonal, Woburn, MA, USA), anti-pan p-Thr287-CaMKII (12-716; Cell Signaling Technology, Danvers, MA, USA), anti-CaMKIIβ (PA5–85747; Thermo Fisher Scientific, Waltham, MA, USA), and goat anti-rabbit IgG-horseradish peroxidase (HRP; AP307P; MilliporeSigma, Burlington, MA, USA). HRP signals were normalized to total protein staining by addition of 2,2,2-trichloroethanol to the resolving gel to calculate relative protein expression between OGTKO and controls as described [27,36,37]. Image analysis was performed in ImageLab (Bio-Rad Laboratories, Hercules, CA, USA) and immunoblot figures are presented as merged files consisting of the chemiluminescent and colorimetric data to show the molecular weight markers.

2.7. SR protein enrichment extraction and calmodulin precipitation

SR-enriched protein lysates were obtained using methods adapted from other work [39]. However, this protocol will likely also result in the enrichment of sarcolemmal membranes [40]. Ventricles from control mice were homogenized in 20 mM HEPES supplemented with 1× HALT EDTA-free protease inhibitor cocktail (87-785; Thermo Fisher Scientific, Waltham, MA, USA), 0.01 calpain inhibitors I and II, 0.001 thiamet G. Lysates were spun at 400 ×*g* to remove debris and nuclei without pelleting myofibrils. The supernatants were spun at 40,000 ×*g* for 30 min and the pellets were resuspended and incubated for 10 min on ice with lysis buffer supplemented with 600 mM KCl. Lysates were spun again at 40,000 ×*g* and resuspended in lysis buffer supplemented with 150 mM NaCl. Protein suspensions were then solubilized with 0.5% amidosulfobentaine and clarified by centrifugation.

For calmodulin precipitation, 500 μg of SR-enriched protein was diluted to 1.5 mgs/ml. This was done in parallel with one aliquot supplemented with 2 mM $CaCl_2$ and the other with 2 mM EGTA. Two 100 μl aliquots of calmodulin-coupled agarose (A6112; Sigma Aldrich, Saint Louis, MO, USA) were washed with SR protein solubilization buffer plus $CaCl_2$ or EGTA. SR-enriched protein was incubated with washed and equilibrated calmodulin for 2 h at 4 °C with end-over-end rotation. Beads were then washed four times with $CaCl_2$- or EGTA-supplemented solubilization buffer, eluted with 1xLDS buffer and 100 mM dithiothreitol at 70 °C for 10 min. Precipitants and supernatants were immunoblotted as described above.

2.8. O-GlcNAc affinity precipitation

Total protein lysates from TCre and OGTKO ventricles were diluted to 1 mg/ml and 1 mg of protein from each group was preabsorbed with streptavidin coated magnetic beads (88-816; Thermo Fisher Scientific, Waltham, MA, USA) for ~1 h at 4 °C. To capture proteins with the O-GlcNAc modification, biotinylated succinylated wheat germ agglutinin (sWGA; B-1025S; Vector Laboratories, Burlingame, CA, USA) was coupled to the streptavidin magnetic beads. Following preabsorption, protein was added to the lectin coupled beads and mixed for 2 h at 4 °C, washed extensively with lysis buffer, and eluted in 1xLDS sample buffer at 60 °C for 10 min. Following elution, eluates were immunoblotted as described above using the anti-CaMKIIδ and anti-CaMKIIβ antibodies.

2.9. Immunofluorescence

Cells were plated on laminin (20 μg/ml) coated coverslips for 1 h at room temperature. Cells were fixed with 4% paraformaldehyde in PBS for 10 min then washed three times with PBS. Cells were permeabilized

and blocked for 30 min in PBS supplemented with 0.3% Triton X-100, 10% goat serum, and 0.2% BSA. Primary antibody incubations were carried out overnight in the refrigerator with rabbit anti-ryanodine receptor 2 (A0298; Abclonal, Woburn, MA, USA) and Alexa Fluor 488 conjugated mouse anti-OGT (sc-74546; Santa Cruz Biotechnology; Dallas, Texas, USA) both at a 1/50 dilution or no primary all in blocking buffer. The next day, cells were washed three times with PBS, incubated with Alexa Fluor 568 conjugated goat anti-rabbit secondary (A11011; Thermo Fisher Scientific, Waltham, MA, USA) for 1 h, then washed again with PBS. Labeled coverslips were mounted on slides with Vectashield Vibrance (H-1800; Vector Laboratories, Newark, CA, USA). Imaging was performed with an Olympus FV1000 confocal microscope using the 488 and 568 lasers for excitation. Analysis was performed with the ImageJ colocalization plugin JACoP according to the developer's recommendations [41].

2.10. Statistical analysis

Data are presented as the mean ± SEM and significance was determined using unpaired student's *t*-tests and Mann-Whitney rank sum tests where appropriate with a p criteria of <0.05. Animal numbers are listed as "N" and cell numbers as "n." All data are available upon reasonable request.

3. Results

3.1. CDF is reduced while Ca_v recovery from inactivation is accelerated in OGTKO cardiomyocytes

To determine the impact of reduced cardiomyocyte O-GlcNAcylation on the dynamic regulation of Ca_v activity, CDF was compared between cardiomyocytes from control and OGTKO mice using a 0.5 Hz repetitive stimulation protocol as described in the Methods. Also, as discussed in the Methods, here and throughout, all control animals for the OGTKO strain were α-MHC-MerCreMer positive, were administered tamoxifen, but possessed a normal OGT gene (referred to as TCre); thereby, controlling for any effects of tamoxifen treatment and Cre expression [34]. Facilitation was observed in both cardiomyocyte types but was significantly reduced in OGTKO cardiomyocytes (Figs.1A and 1B). For example, in control TCre cardiomyocytes, the current elicited from pulse (P) 2 was 131% of the current recorded following P1 while the difference between P2 and P1 currents in OGTKO cardiomyocytes was only 113% (Fig. 1A and B; $N = 3$, $n = 19–23$; $^*p < 0.001$). This amounted to a 58% reduction in OGTKO CDF compared to control TCre CDF.

In addition to I_{Ca} potentiation, CDF may also result in slower Ca_v inactivation, which provides another mechanism for increased Ca^{2+} influx during conditions of repeated depolarizations. In order to compare the effect of CDF on Ca_v inactivation between TCre and OGTKO cardiomyocytes, we measured the time required for the P1 and P2 currents to decay by one exponential unit or to 37% of the peak ($T_{0.37}$) [11] as described in the Methods. The percent change in $T_{0.37}$ between P2 and P1 currents was then calculated and compared. The slowing of P2 current $T_{0.37}$ compared to P1 current was 65% greater in control TCre cardiomyocytes compared to OGTKO cardiomyocytes (Fig. 1D; $N = 3$, $n = 19–23$; $^*p < 0.001$). It should be noted that, as we reported earlier [27] and show here (Fig. 1C), the inherent inactivation rate of OGTKO cardiomyocyte Ca_vs was significantly slower than TCre controls, which can likely be at least partially ascribed to a rightward shift in voltage-dependent activation gating for OGTKO Ca_v [27]. These data indicate that the impact of cardiomyocyte *OGT* ablation on CDF is consistent between the effects on I_{Ca} magnitude and Ca_v inactivation rate.

For reasons detailed in the Methods section, male mice were used in this study. However, to ensure that no sex differences exist in regard to the impact of reduced O-GlcNAcylation on the dynamic regulation of Ca_vs, a subset of experiments were performed on female OGTKO mice. CDF was similarly diminished in cardiomyocytes from female OGTKO

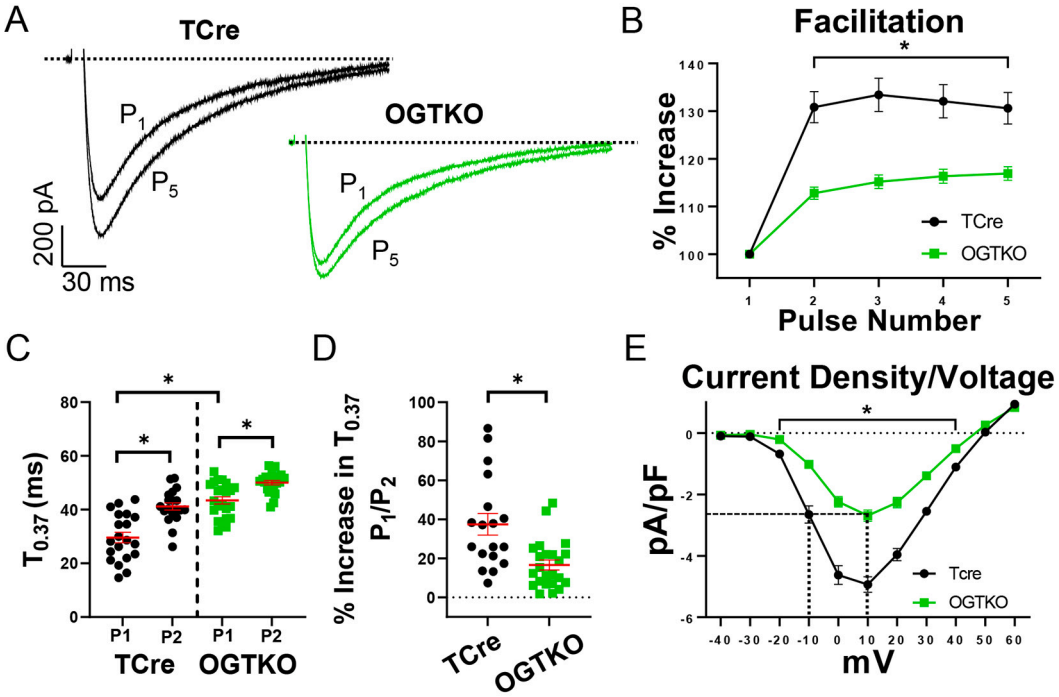

Fig. 1. CDF is reduced in OGTKO cardiomyocytes. A) Representative pulse (P) 1 and P5 current traces from control TCre (black) and OGTKO (light green) cardiomyocytes. B) Percent increases in current compared to P1 current as a function of pulse number. $N = 3$, $n = 19–23$; $^*p < 0.001$. C) The time required for the P1 and P2 currents to decay one exponential unit or to 37% of the peak ($T_{0.37}$). $N = 3$, $n = 19–23$; $^*p \leq 0.001$. D) The percent increase in $T_{0.37}$ between P2 and P1 currents. $N = 3$, $n = 19–23$; $^*p = 0.001$. E) I_{Ca} density-voltage relationships. Dashed lines indicate that the OGTKO I_{Ca} density at a 10 mV test potential is similar to TCre control I_{Ca} density at a − 10 mV test potential. $N = 3$, $n = 22$; $^*p < 0.001$. (For interpretation of the references to colour in this figure legend, the reader is referred to the web version of this article.)

mice compared to female TCre controls (SF1A and SF1B; $N = 2$, $n = 8$–13; $^*p \leq 0.001$). I_{Ca} density was also reduced and voltage-dependent gating was depolarized in female OGTKO cardiomyocytes (SF1C) similar to what was observed in males as shown here (Fig. 1E) and previously [27] indicating that the overall impact of cardiomyocyte *OGT* ablation on Ca_v activity is consistent between the sexes.

3.2. Pharmacologic inhibition of OGT reduces I_{Ca} potentiation during CDF but does not affect the slowing of inactivation

To test whether transient reductions in OGT activity may also impact CDF, we treated cardiomyocytes from wild-type (WT) mice with the cell-permeable OGT inhibitor OSMI-1 [42] or vehicle control (0.1% DMSO) for 1–4 h. CDF was apparent in OSMI-1 and vehicle treated WT cardiomyocytes but was significantly reduced in OSMI-1 treated cardiomyocytes (Fig. 2A and B). The difference in P2 versus P1 currents was 153% in WT vehicle treated cardiomyocytes and 121% in OSMI-1 treated cardiomyocytes (Fig. 2B; $N = 3$–6, $n = 18$–24; $^*p < 0.001$); a 60% reduction in CDF-induced I_{Ca} potentiation. It should be pointed out that CDF was more robust in WT cells than in TCre and OGTKO cells; we currently do not have an unambiguous explanation for this. The WT mice used in this study were ~ 1 month younger than the induced TCre and OGTKO mice; we have some data suggesting that CDF can change with age. Tamoxifen treatment and Cre recombinase expression were also shown to impact cardiomyocyte and heart function including altered gene expression, DNA damage and fibrosis [34,35]. Importantly however, all groups of mice that were compared in this study were age-matched and controlled for tamoxifen induction and Cre expression.

In contrast to what was observed in OGTKO cardiomyocytes (Fig. 1D), OSMI-1 treatment did not impact Ca_v inactivation compared to controls when comparing P2 versus P1 currents. $T_{0.37}$ was calculated as described in the Methods and done in Fig. 1C and D and showed that the percent increase in P2 versus P1 inactivation was statistically similar between vehicle treated WT cardiomyocytes and OSMI-1 treated cardiomyocytes (Fig. 2D; $N = 3$–6; $n = 18$–24; $p = 0.9$). Interestingly, we also observed no inherent slowing of Ca_v inactivation following OSMI-1 treatment (Fig. 2C; $N = 3$–6; $n = 18$–24; $p = 0.6$) as was observed in OGTKO cardiomyocytes (Fig. 1C and [27]) indicating that the impact of OGT inhibition on Ca_v activity by OSMI-1 is incomplete compared to *OGT* ablation or that ablation is accompanied by additional cellular remodeling.

3.3. Ca_v recovery from inactivation is slowed in OSMI-1 treated cardiomyocytes but not in OGTKO cardiomyocytes

Recovery from inactivation is another dynamic property of Ca_vs that is crucial for proper EC coupling at higher heart rates. Like the effects on CDF, CaMKII activity was shown to accelerate Ca_v recovery [5,11,43–45]. Based on the similarities between the effects of CaMKII inhibition and OGT inhibition on CDF, we hypothesized that Ca_v recovery would be consistently slowed in OGTKO cardiomyocytes. This, however, was not the case: Ca_v recovery from inactivation was in fact 29% faster in OGTKO cardiomyocytes than in controls (Fig. 3A; $N = 3$, $n = 22$; $^*p < 0.001$), which was compared using the time constants (Tau) generated from fitting the recovery curves with a mono-exponential function as described in the Methods. Recovery from inactivation is a more complex process than CDF in that not only is it affected by CaMKII activity but is also impacted by voltage- and Ca^{2+}-dependent inactivation (CDI) and intracellular Ca^{2+} [11,43]. As we reported previously [27] and here (Fig. 1E), I_{Ca} density and intracellular Ca^{2+} release were both reduced in OGTKO cardiomyocytes. At a test potential of 10 mV, which was the test potential used to measure CDF and recovery, OGTKO I_{Ca} density was reduced by 40% compared to controls (Fig. 1E; $N = 3$, $n = 22$; $^*p < 0.001$). As denoted with the dashed lines in Fig. 1E, at a test potential of −10 mV, control I_{Ca} density was similar to OGTKO I_{Ca} density at 10 mV. Data from work by others suggests that while CaMKII acts to accelerate Ca_v recovery from inactivation, intracellular Ca^{2+} slows recovery [11]. Thus, to question whether the acceleration in OGTKO Ca_v recovery from inactivation, despite the reduction in CDF, could be ascribed to a reduction in Ca^{2+} influx and/or Ca^{2+}-induced Ca^{2+}-release, we compared Ca_v recovery in a subset of control TCre cardiomyocytes at test potentials of −10 mV and 10 mV. At a test potential of −10 mV, control Ca_v recovery was accelerated by 32% compared to recovery at a 10 mV test potential (Fig. 3B; $N = 2$, $n = 9$; $^*p < 0.001$). These data suggest that the acceleration in OGTKO Ca_v recovery is due to a reduction in Ca^{2+} entry and/or Ca^{2+}-induced Ca^{2+}-release. If a reduction in Ca^{2+} entry/release similarly affected CDF, this would be a trivial explanation for the observed reduction in OGTKO CDF (Fig. 1A and B). To test this, CDF was also compared at the two test potentials in control cardiomyocytes. Despite the reduced I_{Ca}, CDF was increased by 18% at the −10 mV test potential (P2 versus P1 currents) compared to CDF at the 10 mV test potential (Fig. 3C; $N = 2$, $n = 8$; $^*p = 0.01$). The reason for the increase in facilitation at −10 mV compared to

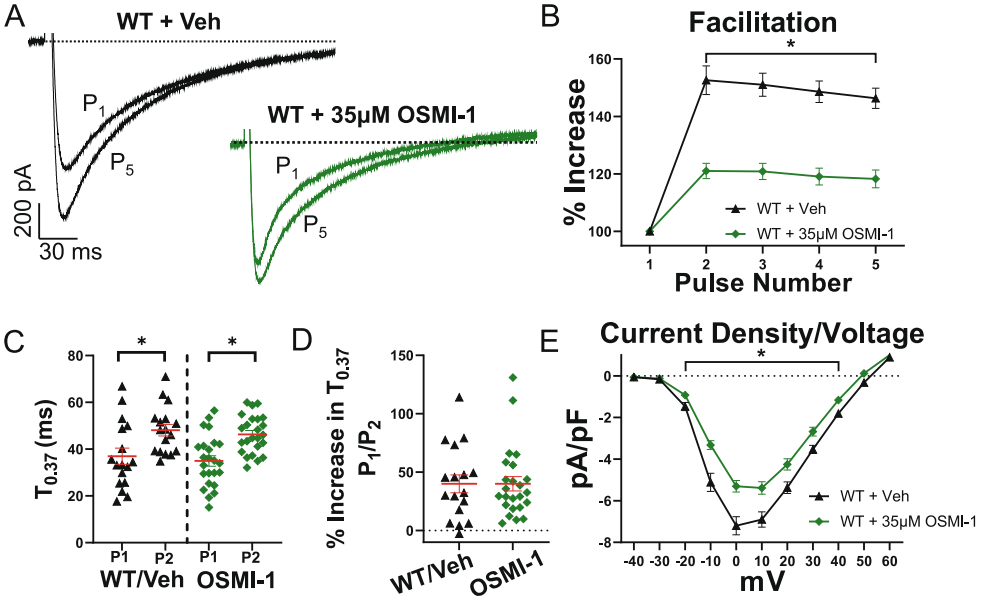

Fig. 2. Transient inhibition of OGT from OSMI-1 treatment reduces CDF-induced I_{Ca} potentiation but does not impact inactivation. A) Representative P1 and P5 current traces from control vehicle treated (black) and OSMI-1 treated (dark green) cardiomyocytes. B) Percent increases in current compared to P1 current as a function of pulse number. $N = 3$–6, $n = 18$–24; $^*p < 0.001$. C) The time required for the P1 and P2 currents to decay one exponential unit or to 37% of the peak ($T_{0.37}$). $N = 3$–6, $n = 18$–24; $^*p \leq 0.01$. D) The percent increase in $T_{0.37}$ between P2 and P1 currents. $N = 3$–6, $n = 18$–24; $p = 0.9$. E) I_{Ca} density-voltage relationships. $N = 3$–6, $n = 19$–25; $^*p \leq 0.01$. (For interpretation of the references to colour in this figure legend, the reader is referred to the web version of this article.)

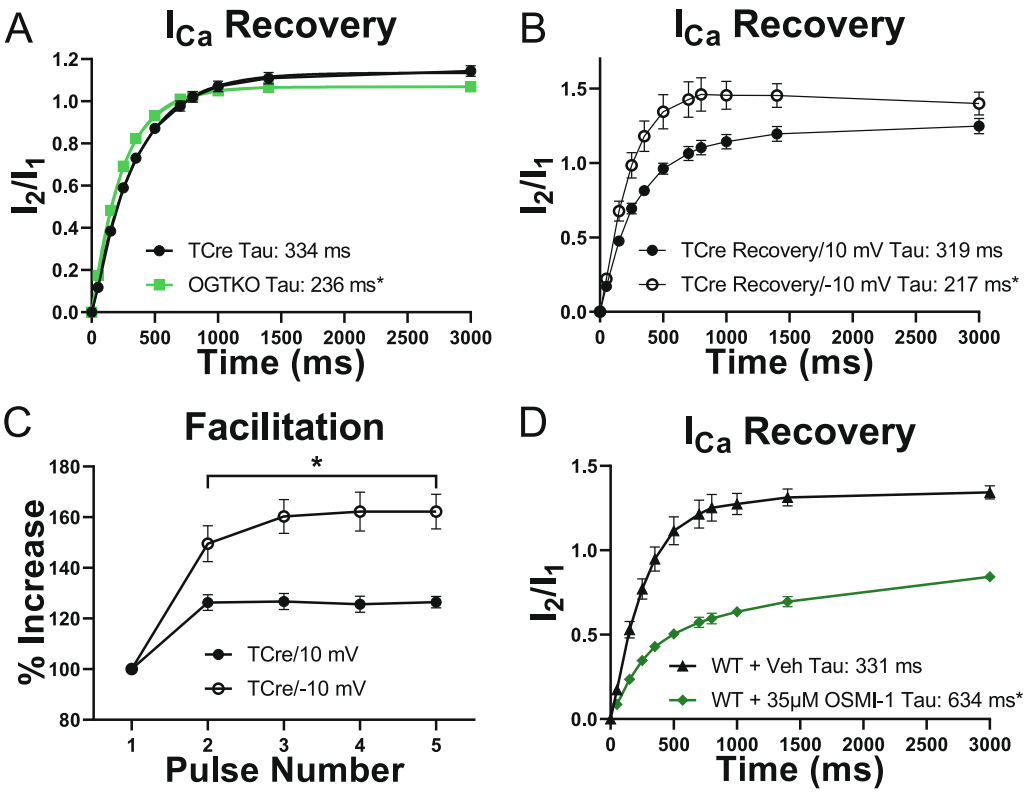

Fig. 3. Ca_v recovery from inactivation is accelerated in OGTKO cardiomyocytes, which is likely a result of reduced I_{Ca} and/or Ca^{2+}-induced Ca^{2+}-release, but recovery is slowed in OSMI-1 treated cardiomyocytes. A) Ca_v recovery from inactivation was fit with a mono-exponential function and was accelerated in OGTKO cardiomyocytes. $N = 3$, $n = 22$; $^*p < 0.001$. B) Ca_v recovery in control cardiomyocytes is accelerated to a similar degree as recovery in OGTKO cardiomyocytes when I_{Ca} is reduced due to a smaller depolarization (−10 mV versus 10 mV). $N = 2$, $n = 9$; $^*p = 0.001$. C) CDF in TCre control cardiomyocytes at test potentials of −10 and 10 mV. $N = 2$, $n = 8$; $^*p \leq 0.01$. D) Ca_v recovery from inactivation was fit with a mono-exponential function and was slowed in OSMI-1 treated cardiomyocytes. $N = 3$, $n = 12–14$; $^*p < 0.001$.

10 mV is not known at this time but may be a result of less CDI elicited by the smaller depolarization or simply due to the way in which the facilitation was measured (i.e., if at some point CDF reaches a steady-state that is largely independent of the initial I_{Ca} magnitude then a smaller depolarization and thus a smaller initial current would decrease the denominator used in the CDF calculation). Nevertheless, unlike the impact of intracellular Ca^{2+} on recovery in OGTKO cardiomyocytes, these data strongly suggest that the reduction in OGTKO I_{Ca} density is not directly responsible for the reduced CDF.

In contrast to the acceleration of Ca_v recovery from inactivation observed in OGTKO cardiomyocytes (Fig. 3A), recovery in WT OSMI-1 treated cardiomyocytes was slowed by ~two-fold (Fig. 3D; $N = 3$, $n = 12–14$; $^*p < 0.001$). These findings are consistent with the slowing of Ca_v recovery from inactivation following CaMKII inhibition [5,11,43–45]. Ca_v recovery in WT vehicle treated cardiomyocytes also demonstrated an overshoot of current at recovery intervals of 500 ms and greater (Fig. 3D), which can likely be attributed to CDF although this overshoot of current will not be equivalent to CDF because of an accumulation of inactivated Ca_vs caused by the initial high-frequency depolarizations of the recovery protocol [46]. Similar to what was reported in conditions of CaMKII inhibition [43], this overshoot was abolished in WT OSMI-1 treated cardiomyocytes. In fact, recovery failed to reach P1 current levels even at a recovery interval of 3 s in conditions of acutely reduced OGT activity (Fig. 3D), which was likely a result of a greater accumulation of inactivated Ca_vs caused by the slower recovery time. At a 10 mV test potential, I_{Ca} density was ~20% lower in OSMI-1 treated cardiomyocytes (Fig. 2E; $N = 3–6$, $n = 19–25$; $^*p = 0.003$); however, this was apparently too small a reduction in I_{Ca} to cause an acceleration in Ca_v recovery as observed in OGTKO cardiomyocytes (Fig. 3A). This may be due to the fact that the relationship between I_{Ca} and Ca^{2+}-induced Ca^{2+}-release is saturating [47]. Consistently, as will be discussed in the next section, at 0.5 Hz, Ca^{2+}-induced Ca^{2+}-release was not impacted by OSMI-1 treatment. It is also possible that OSMI-1 treatment potentiates Ca^{2+}-induced Ca^{2+} release despite the marginal reduction in I_{Ca} (Fig. 2E).

3.4. Inhibition of global Ca^{2+} release by high Ca^{2+} buffering abolishes CDF in OGTKO and OSMI-1 cardiomyocytes

I_{Ca} triggers Ca^{2+} release from the SR via ryanodine receptors resulting in whole-cell Ca^{2+} waves [1]. This whole-cell rise in intracellular Ca^{2+} can impact Ca_v function including CDF, recovery from inactivation and Ca^{2+}-dependent inactivation [11,48–51]. To determine whether cardiomyocyte *OGT* ablation (OGTKO) and/or OGT inhibition (OSMI-1) alter the effects of SR-mediated whole-cell Ca^{2+} release on CDF and Ca_v recovery from inactivation, the concentration of the Ca^{2+} chelator EGTA was raised to 10 mM and Ca^{2+} was omitted from the intracellular recording solution. As discussed in the Methods, at 10 mM intracellular EGTA, Ca^{2+} accumulation would likely only occur at the mouth of the channel and whole-cell increases in intracellular Ca^{2+} would be prevented [3,5,9,48]. CDF and Ca_v recovery from inactivation shown in Figs. 1–3, were recorded with 1 mM Ca^{2+} and 5 mM EGTA in the intracellular solution. At these concentrations, resting intracellular Ca^{2+} was calculated to be at a closely physiologic level of approximately 80 nM (calculated using Schoenmakers' chelator algorithm, which accounts for ATP and Mg^{2+} [52]). In the presence of 10 mM intracellular EGTA and nominally Ca^{2+} free, CDF-induced I_{Ca} potentiation was diminished in control TCre cardiomyocytes and abolished in OGTKO cardiomyocytes (SF2A and SF2B; $N = 3$, $n = 11–12$; $^*p \leq 0.02$). The impact of CDF on Ca_v inactivation was also diminished in control TCre cardiomyocytes and abolished in OGTKO cardiomyocytes (SF2D; $N = 3$, $n = 11–13$; $^*p = 0.03$). Consistent with the acceleration of OGTKO Ca_v recovery from inactivation shown in Fig. 3A, OGTKO Ca_v recovery from inactivation was still accelerated with 10 mM intracellular EGTA compared to controls (SF2E; $N = 3$, $n = 11–12$; $^*p = 0.001$).

CDF-induced I_{Ca} potentiation was also diminished in vehicle-treated WT cardiomyocytes and abolished in OSMI-1 treated cardiomyocytes with 10 mM intracellular EGTA and nominally Ca^{2+} free (SF3A and SF3B). Cells treated with OSMI-1 also demonstrated I_{Ca} depression of ~9–12% during the CDF protocol with 10 mM EGTA in the patch pipette (SF3A and SF3B, $N = 3$, $n = 17–19$; $^*p < 0.0001$). Depression of I_{Ca}

current during repeated depolarizations was also reported in conditions of SR-targeted CaMKII inhibition [5] and others have suggested that depression occurs simultaneously with CDF and is Ca^{2+} sensitive but not Ca^{2+} dependent [53]. If depression is Ca^{2+} sensitive, the lack of depression observed in OGTKO cardiomyocytes with 10 mM intracellular EGTA may be a result of the marked reductions in I_{Ca} and SR Ca^{2+} release in these cells (Fig. 1E and [27]) or an inherent difference of Ca^{2+} sensitivity resulting from *OGT* ablation compared to transient OGT inhibition (OSMI-1 treatment).

In pseudo-physiologic conditions (1 and 5 mM intracellular Ca^{2+} and EGTA respectively), we observed no difference in the percent change of P2 versus P1 inactivation rates between vehicle treated WT and OSMI-1 treated cardiomyocytes (Fig. 2D). However, when the intracellular recording solution was nominally Ca^{2+} free and contained 10 mM EGTA, the mean percent change of the P2 versus P1 current inactivation rate ($T_{0.37}$) was ~43% higher in vehicle-treated WT cardiomyocytes versus OSMI-1 treated myocytes (SF3D; $N = 3$, $n = 17–19$; $^*p = 0.02$). Ca_v recovery from inactivation was still significantly slower in OSMI-1 treated cardiomyocytes in the presence of 10 mM EGTA compared to controls (SF3E; $N = 3$, $n = 17–19$; $^*p < 0.001$. Taken together, these data suggest that in conditions of reduced O-GlcNAcylation, the regulation of Ca_vs by intracellular Ca^{2+} is diminished.

To directly investigate the impact of SR Ca^{2+} release on CDF and Ca_v recovery from inactivation, 2 μM ryanodine was included in the extracellular recording solution as described in the Methods. Ryanodine abolished CDF-induced I_{Ca} potentiation, resulting in depression, and the slowing of inactivation and significantly slowed recovery from inactivation in vehicle treated WT cardiomyocytes (SF4A-SF4E; $N = 3$, $n = 6–18$; $^*p \leq 0.001$). Based on these experiments, SR Ca^{2+} release is necessary for CDF and accelerates Ca_v recovery from inactivation, which is consistent with work by others [11,48,49,54]. Some, however, have reported no effect of ryanodine on CDF [46,55] although dose and incubation time may contribute to the discrepancy of these studies. The data reported here also strongly suggest that 10 mM intracellular EGTA does not abolish SR Ca^{2+} release but likely results in only its accumulation in the dyad space near the mouth of Ca_vs.

3.5. FDAR is reduced in conditions of chronic (OGTKO) and acute (OSMI-1 treated) reductions in OGT activity

To compare FDAR among the different conditions of reduced OGT activity (OGTKO and OSMI-1 treated cardiomyocytes), whole-cell Ca^{2+} transients were recorded from field-stimulated fura-8 loaded cells at 0.5 and 3 Hz. FDAR was measured as the percent increase in acceleration rate of the Ca^{2+} transient decay (reduced time constant, Tau) at the higher versus lower stimulation frequency and was observed in all groups (Fig. 4A and B). However, FDAR was significantly smaller in OGTKO and OSMI-1 treated cardiomyocytes compared to their respective controls (Fig. 4A and C). In TCre cardiomyocytes, the Ca^{2+} transient rate of decay (measured as time constant Tau, the inverse of rate) was accelerated by 39% when cardiomyocytes were stimulated at 3 Hz versus 0.5 Hz; Ca^{2+} transient decay was only accelerated by 23% in OGTKO cardiomyocytes (Fig. 4A and C; $N = 3$, $n = 24–39$; $^*p < 0.001$). In vehicle treated WT cardiomyocytes, the Ca^{2+} transient decay was accelerated by 46% when increasing the stimulation frequency to 3 Hz from 0.5 Hz; in OSMI-1 treated WT cardiomyocytes, the decay rate was only accelerated by 35% (Fig. 4C; $N = 3$, $n = 28–34$; $^*p = 0.002$). Consistent with our previous data [27], the Ca^{2+} transient amplitude was reduced by 45% in OGTKO cardiomyocytes at 0.5 Hz and 3 Hz (data not shown; $N = 3$, $n = 24–39$; $^*p < 0.001$). At 0.5 Hz, Ca^{2+} transient amplitudes were similar between vehicle and OSMI-1 treated WT cardiomyocytes. However, at 3 Hz, Ca^{2+} transient amplitude was reduced by 35% in OSMI-1 treated cardiomyocytes (data not shown; $N = 3$, $n = 28–34$; $^*p < 0.001$).

3.6. CaMKII autophosphorylation is markedly reduced in OGTKO ventricles despite increased expression of CaMKIIδ and calmodulin

To explore the molecular mechanism for the reduction in CDF and FDAR we assessed CaMKII and calmodulin expression and CaMKII autophosphorylation in control TCre and OGTKO ventricles by immunoblot. CaMKIIδ expression, the predominate CaMKII isoform in the heart [14,15], was increased 1.7-fold in OGTKO ventricles (Fig. 5A and E; $N = 4$; $^*p < 0.001$). Calmodulin expression was also increased in OGTKO ventricles, although to a lesser extent than CaMKIIδ (1.3-fold; Fig. 5B and E; $N = 5–7$; $^*p = 0.01$). Inter-subunit CaMKII autophosphorylation at Thr287 (Thr286 in the α isoform) is an important regulatory mechanism that can increase CaMKII's affinity for Ca^{2+}/calmodulin and generate autonomous activity [56]. We next questioned whether CaMKII autophosphorylation was altered in the ventricles of OGTKO mice using a pan anti-phospho-Thr287(Thr286) CaMKII specific antibody. Immunoblotting with this antibody generated two bands at

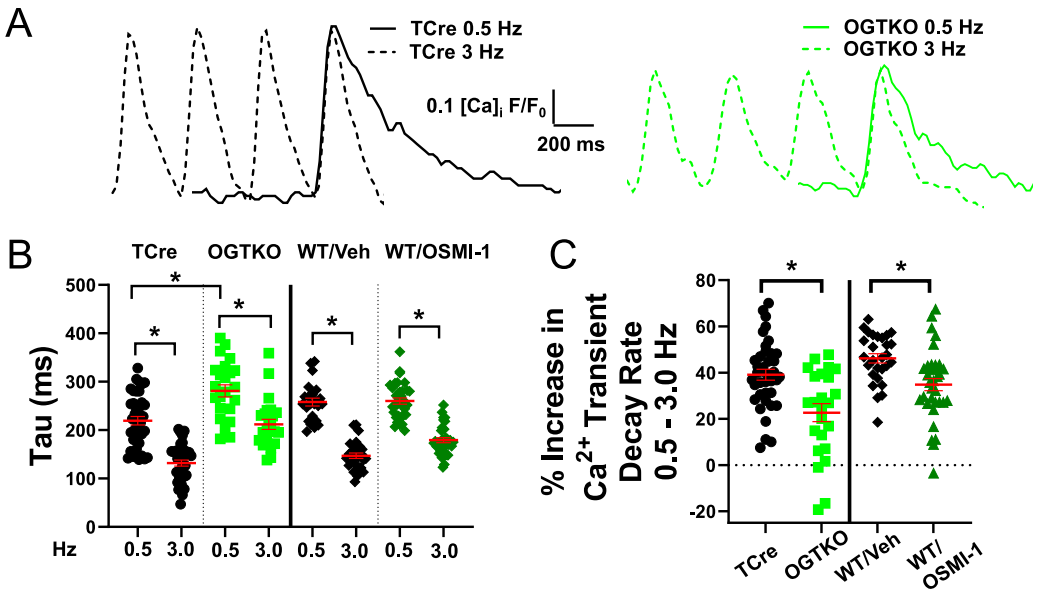

Fig. 4. FDAR is reduced in OGTKO and OSMI-1 treated cardiomyocytes. A) Representative Ca^{2+} transients from control TCre (black) and OGTKO (light green) cardiomyocytes at stimulation frequencies of 0.5 (solid lines) and 3 Hz (dashed lines). B) Ca^{2+} transient inactivation time constants (Tau) at 0.5 and 3 Hz. $N = 3$, $n = 24–39$; $^*p < 0.001$ under conditions of chronic (OGTKO; light green) or acute (OSMI-treatment; dark green) OGT inhibition versus controls (black). C) Percent increases in Ca^{2+} transient decay rate when stimulation frequency increased from 0.5 to 3 Hz. $N = 3$, $n = 24–39$; $^*p \leq 0.002$. Indicating that the increase in Ca^{2+} transient decay rate when stimulation frequency increased (0.5 versus 3.0 Hz) was significantly reduced in OGTKO and OSMI-1 treated cardiomyocytes versus their respective controls. (For interpretation of the references to colour in this figure legend, the reader is referred to the web version of this article.)

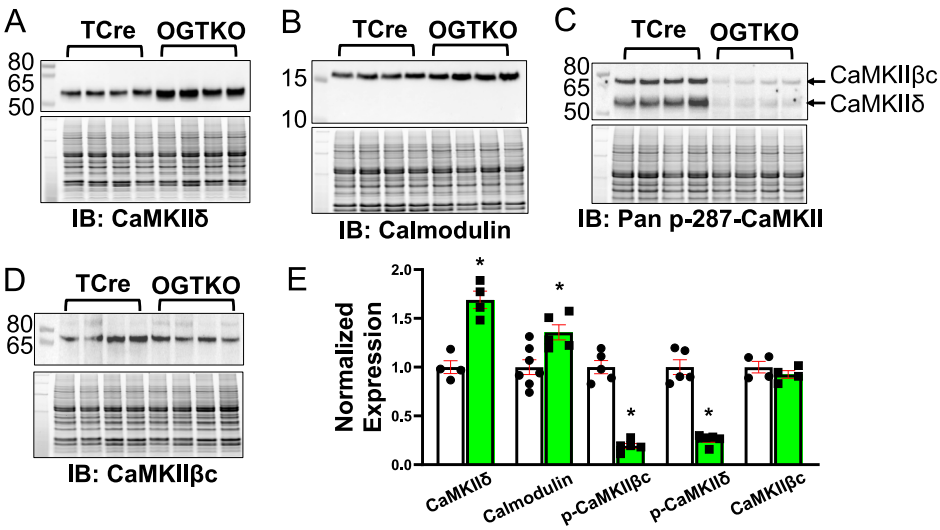

Fig. 5. CaMKII autophosphorylation is reduced by at least 75% in OGTKO ventricles despite increased expression of CaMKIIδ and calmodulin. A-D) Immunoblots (IBs; top panels) and total protein (bottom panels) showing CaMKIIδ (A), calmodulin (B), pan p-Thr287-CaMKII (C), and CaMKIIβc (D) expression in control TCre and OGTKO ventricles. E) IB signals were normalized to total protein levels and signals were compared between TCre (white bars) and OGTKO (light green bars). $N = 4–7$; $*p \leq 0.01$. (For interpretation of the references to colour in this figure legend, the reader is referred to the web version of this article.)

~72 and ~55 kD (Fig. 5C), with the 55 kD band likely representing autophosphorylated CaMKIIδ and to a lesser extent CaMKIIγ. The 72 kD band was indicative of the novel CaMKIIβ isoform found in skeletal (CaMKIIβs) and cardiac (CaMKIIβc) muscle that contains an ~12 kD polypeptide insert in the variable region and that is sequestered to the SR by the CaMKII-related protein αKAP [57–60]. Autophosphorylation of the ~55 kD (likely, CaMKIIδ) and ~72 kD (likely, CaMKIIβc) proteins was nearly abolished in OGTKO ventricles (75 and 81% respectively; Fig. 5C and E; $N = 5$; $*p < 0.0001$). When considering that CaMKIIδ expression was increased 1.7-fold in OGTKO ventricles, the reduction in OGTKO CaMKIIδ autophosphorylation is even more striking. To verify that CaMKIIβc was present in these samples, immunoblot was performed using an anti-CaMKIIβ antibody raised against an epitope away from the variable region. CaMKIIβc expression was not different between OGTKO and TCre control ventricles (Fig. 5D and E; $N = 4$; $p = 0.3$).

3.7. OGT is likely enriched in the dyad space and/or at the SR and binds to calmodulin in a Ca^{2+}-dependent manner

If OGT is exerting a direct effect on the CDF machinery, it would likely need to be spatially coupled to Ca_Vs, CaMKII, calmodulin, or some combination of the three. In support of this, using proximity ligation proteomics, others have shown that OGT is in close proximity to $Ca_V\alpha1$ and $Ca_V\beta2$ [61]. To further explore whether OGT is colocalized with CDF-related proteins found in the dyad space and/or at the SR, we performed pull-down experiments with SR-enriched protein lysates using calmodulin-coupled agarose. The calmodulin pull-downs were performed in parallel with one aliquot containing $CaCl_2$ and the other

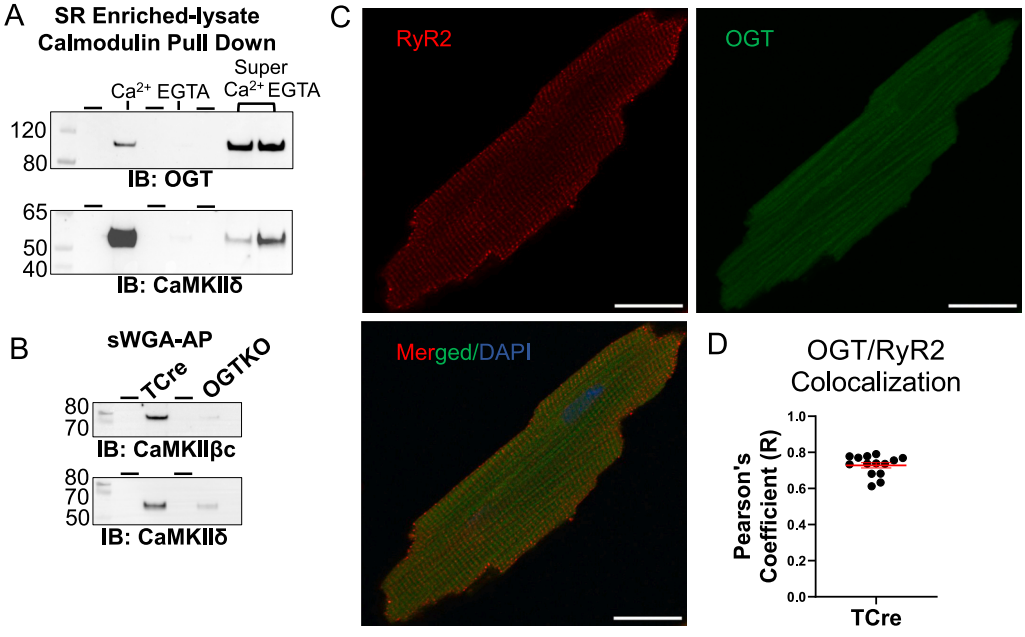

Fig. 6. SR-enriched OGT precipitates with calmodulin in a Ca^{2+}-dependent manner, CaMKIIβc is likely O-GlcNAcylated, and OGT colocalizes with ryanodine receptors. A) SR-enriched lysates were precipitated with calmodulin-agarose with Ca^{2+} or EGTA present. The eluents were immunoblotted and blots were probed with anti-OGT (top) and anti-CaMKIIδ (bottom) antibodies. The dashes at the top of the blots represent lanes that were left blank to prevent carry-over among lanes if a large volume was required for loading. The lanes labeled as "Super" represent the supernatants from the calmodulin precipitation in the two conditions. B) Protein lysates from TCre control and OGTKO ventricles were affinity purified (AP) with the GlcNAc-specific lectin sWGA. Eluates were immunoblotted with anti-CaMKIIβ (top panel) and anti-CaMKIIδ (bottom panel) antibodies. A and B represent data from at least 2 independent experiments. C) Confocal images of fixed and permeabilized cardiomyocytes that were immunolabeled with an Alexa Fluor 488 conjugated anti-OGT antibody (green) and an anti-ryanodine receptor antibody. Ryanodine receptors were visualized with an Alexa Fluor 568 conjugated anti-rabbit secondary (red). D) Scatter plot showing Pearson's correlation coefficient (R) values and mean of 0.73 ± 0.01 ($N = 2$, $n = 14$) indicating significant colocalization of OGT and ryanodine receptors. Scale bars indicate 20 μm. (For interpretation of the references to colour in this figure legend, the reader is referred to the web version of this article.)

containing EGTA as described in the Methods. Ca^{2+} binding by calmodulin exposes several hydrophobic regions with which a variety of calmodulin-binding proteins can interact, this interaction typically indicates a functional relationship between calmodulin and the protein of interest that is Ca^{2+} dependent as is CDF and FDAR. Following pull-down, proteins were eluted with heat in sample buffer and Western blotted. As seen in the top panel of Fig. 6A, immunoblotting showed that SR-enriched OGT is bound to calmodulin in a Ca^{2+} dependent manner. Fig. 6A bottom panel shows the lower portion of the blot that was probed with an anti-CaMKIIδ antibody demonstrating the specificity of the experiment. Others have shown that CaMKIIβc also is precipitated by calmodulin in a Ca^{2+} dependent manner in cardiac SR-enriched lysates [58]. Together, these data suggest that OGT is a component of an SR-related signaling complex that contributes to the regulation of Ca^{2+} handling.

The Bers group showed that CaMKIIδ was O-GlcNAcylated at Ser280 [28] and at Ser279 in CaMKIIα [29]. CaMKIIβ possesses a similar Ser in its regulatory domain [29]. To determine if CaMKIIβc could also be O-GlcNAcylated and demonstrate that the O-GlcNAcylation of CaMKIIδ and CaMKIIβc was reduced in OGTKO ventricles, we performed affinity precipitation using the GlcNAc-specific lectin succinylated wheat germ agglutinin (sWGA) as in our previous efforts [27]. Following immunoblotting, it was apparent that CaMKIIβc could be successfully precipitated by sWGA strongly suggesting that, like the other CaMKII isoforms, it too can be O-GlcNAcylated (Fig. 6B). Not surprisingly, we also observed that sWGA pulled down ~5 to 20 times more CaMKIIδ and CaMKIIβc respectively from TCre control ventricular lysates compared to OGTKO lysates (Fig. 6B)

OGT has traditionally been considered a nucleocytoplasmic protein. Our functional data indicate that OGT impacts CDF and FDAR (Figs. 1–4), which are processes that occur at the SR and/or dyad space, and our biochemical data (Fig. 6A) indicate that OGT can also associate with cellular membranes including likely SR membranes. To provide additional evidence for an association of OGT with SR membranes and/or within the dyad space, immunofluorescence of isolated cardiomyocytes using an antibody specific for the cardiac ryanodine receptor (RYR2), which is only found at the SR, and an Alexa Fluor 488 conjugated anti-OGT antibody were used to determine colocalization. Ryanodine receptors were visualized with an Alexa Fluor 568 conjugated anti-rabbit secondary. Data were processed using the ImageJ JACoP plugin as described in the Methods and indicated a mean ± SEM Pearson's correlation coefficient (R) of 0.73 ± 0.014 ($N = 2$; $n = 14$) indicating significant overlap of the OGT and RYR2 fluorescence signal (Fig. 6C and D). Taken together, our data suggest that OGT can associate with the SR and/or reside within the dyad space to impact CDF and FDAR.

3.8. CDF following OGT inhibition is more sensitive to omission of exogenous ATP

The function of CaMKIIβc in cardiomyocytes is not well understood. In the heart, it is tethered to the SR and colocalizes with calmodulin and SERCA2a with the latter interaction likely occurring through αKAP [58]. In vitro, CaMKIIβc can phosphorylate SERCA2a and regulate SR-associated GAPDH activity suggesting that it may regulate ATP generation at the SR [58–60]. All glycolytic enzymes can be found in association with cardiac and skeletal muscle SR vesicles where they produce ATP and are functionally coupled to SR Ca^{2+} transport [60,62,63]. Additionally, ATP generation, likely as a substrate for Ca_v phosphorylation by CaMKII, is an important component of CDF as evidenced by the fact that when a non-hydrolysable form of ATP is included in an intracellular recording solution, CDF is abolished [8]. Given the role of OGT as a nutrient-sensor and the fact that CaMKIIβc autophosphorylation was nearly abolished in OGTKO ventricles (Fig. 5C and E), we were interested in whether one potential role for OGT in CDF was to contribute to the regulation of ATP generation at the SR and/or the dyad space. This line of questioning is also consistent with the data generated by others indicating that SR-targeted CaMKII inhibition abolishes CDF and reduces FDAR [5] highlighting the importance of the SR, and likely the dyad space, to the dynamic regulation of Ca_vs. The intracellular recording solution used to measure CDF depicted in Figs. 1 and 2 contained 5 mM ATP. In a subset of experiments, we replaced ATP with an isomolar amount of aspartic acid, then compared CDF between vehicle and OSMI-1 treated WT cardiomyocytes. In these conditions, all ATP would need to come from existing pools or be generated during the repeated depolarization protocol. Without exogenous ATP, CDF in vehicle treated WT cardiomyocytes was reduced by 36% compared to when 5 mM ATP was present in the patch pipette (from 153% to 134%; comparing the change in P2 versus P1 currents) (Fig. 7; $N = 3$, $n = 18$; $^*p = 0.004$). CDF in OSMI-1 treated WT cardiomyocytes was reduced by 52% (from 121% to 110%) following removal of exogenous ATP (Fig. 7; $N = 3–6$, $n = 14–24$; $^*p = 0.02$). These data highlight the importance of ATP to CDF. Additionally, since OSMI-1 treated cardiomyocytes were more sensitive to removal of exogenous ATP, the data also suggest that a defect in SR-related ATP generation due to reduced OGT activity may contribute to the reductions in CDF and FDAR observed in OGTKO and OSMI-1 treated cardiomyocytes.

4. Discussion

4.1. Reduced OGT activity contributes to CDF and FDAR likely through inhibition of CaMKII autophosphorylation and activity

CDF and FDAR are important adaptive processes that allow the heart to function efficiently when heart rate increases. CaMKII was shown to be responsible for CDF and, at a minimum, contribute to FDAR

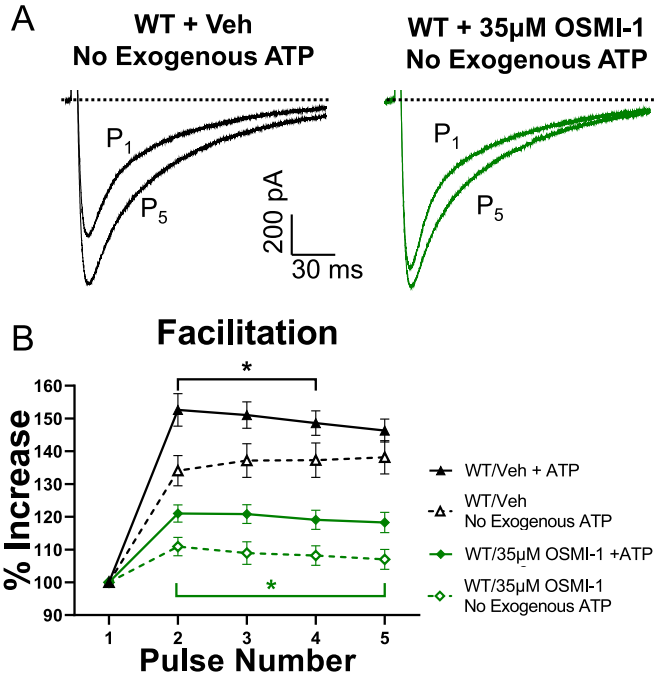

Fig. 7. CDF following OGT inhibition is more sensitive to omission of exogenous ATP. A) Representative P1 and P5 current traces from control vehicle treated (black) and OSMI-1 treated (dark green) cardiomyocytes in the absence of exogenous ATP. B) Percent increases in current compared to P1 current as a function of pulse number. The facilitation curves show that CDF is reduced to a greater extent in OSMI-1 treated cardiomyocytes than controls when exogenous ATP (dashed lines) is removed. Facilitation curves generated with 5 mM ATP in the patch pipette (solid lines) are from Fig. 3B. $N = 3–6$, $14–24$; $^*p \leq 0.02$. (For interpretation of the references to colour in this figure legend, the reader is referred to the web version of this article.)

[5,6,8,10,64]. In the present study, we show that OGT also contributes to these processes demonstrating how multiple signaling pathways and potentially metabolism may converge to regulate cardiomyocyte Ca^{2+} handling. While our previous work suggests that $Ca_v\alpha1.2$, $Ca_v\beta2$, or both subunits can be O-GlcNAcylated [27], it is unlikely that a direct modification of Ca_vs by OGT contributes to CDF since SR-targeted CaMKII inhibition abolished CDF [5], indicating that OGT impacts CDF indirectly. The responsible mechanism, at least in part, likely involves the observed >75% reductions in CaMKII autophosphorylation, despite increased CaMKIIδ and calmodulin expression, when *OGT* is ablated (Fig. 5B, C, and E). While autophosphorylated CaMKII is considered to be autonomously active, autophosphorylation does not exclude CaMKII from further activation by Ca^{2+}/calmodulin [65]. Since the binding of Ca^{2+}/calmodulin to CaMKII is enhanced when CaMKII is autophosphorylated [56], it is likely that during high frequency depolarizations, autophosphorylated CaMKII plays an important role in the rapid response of CDF. Therefore, in conditions of reduced OGT activity, where CaMKII autophosphorylation is reduced, there would be a smaller pool of readily activatable CaMKII. The precise mechanism for the reduction in CaMKII autophosphorylation in conditions of reduced O-GlcNAcylation is not known at this time. A trivial explanation would be that the reduced I_{Ca} current and Ca^{2+}-induced Ca^{2+}-release observed in OGTKO cardiomyocytes results in less Ca^{2+} binding to calmodulin and therefore less activation of CaMKII. However, this likely could not explain how transient inhibition of OGT from OSMI-1 treatment, were I_{Ca} is only marginally reduced and Ca^{2+}-induced Ca^{2+}-release is only affected at a high stimulation frequency (higher than the frequency used to assess CDF and recovery from inactivation), can confer a similar phenotype as *OGT* ablation, where I_{Ca} and Ca^{2+}-induced Ca^{2+}-release are drastically reduced (Fig. 2B and [27]). It should also be pointed out that the amplitude of the fura-8 ratio during diastole (before and between stimulations) was not different in any group (data not shown) suggesting that *OGT* ablation or OGT inhibition does not impact steady-state intracellular Ca^{2+} levels. The most likely potential explanations for the effect of OGT on CaMKII autophosphorylation include: 1) there are unidentified O-GlcNAc sites in addition to Ser280 (Ser279) on CaMKII that regulate autophosphorylation, 2) O-GlcNAcylation or OGT impacts CaMKII's binding of Ca^{2+}/calmodulin, 3) another protein that is regulated by OGT contributes to the regulation of CaMKII autophosphorylation, and/or 4) CaMKII O-GlcNAcylation increases the duration of CaMKII activation and/or the number active monomers within the holoenzyme, both of which would lead to more CaMKII autophosphorylation. Based on the data using 10 mM intracellular EGTA (SF2-SF3) suggesting that in conditions of reduced O-GlcNAcylation, the regulation of Ca_vs by intracellular Ca^{2+} is diminished, another possibility is that OGT impacts CaMKII activity and autophosphorylation indirectly. This may occur through a change in the sensitivity of calmodulin to Ca^{2+} which could then directly impact CaMKII activation or indirectly impact CaMKII by altering the activity of protein phosphatases responsible for removing CaMKII's autophosphorylation such as calcineurin and protein phosphatase 1 [66,67] These potential mechanisms are currently under investigation.

4.2. A potential role for OGT-mediated regulation of CaMKIIβc in CDF and FDAR

CaMKIIδ is likely the major contributor to CDF but whether it's solely responsible is not known. The initial studies identifying the link between CaMKII and CDF used pharmacologic approaches and those drugs have no isoform specificity [7–9]. Additionally, prior work by others showed that CDF was only ~20% lower in cardiomyocytes from mice where the CaMKIIδ gene was ablated compared to controls [16]. This would suggest, at a minimum, that other CaMKII isoforms are able to contribute to CDF. Because SR-targeted CaMKII inhibition abolished CDF and reduced FDAR [5], the SR-targeted CaMKIIβc is a good candidate to contribute to these processes. Additionally, the mechanism responsible for FDAR is still under debate although it is widely considered to involve an increase in SERCA2a V_{max} with some providing data for and others against the notion that this involves phosphorylation of SERCA2a by CaMKII [68–71]. CaMKIIβc can phosphorylate SERCA2a in vitro indicating that if FDAR requires SERCA2a phosphorylation, CaMKIIβc may be involved. CaMKIIβc also likely contributes to ATP generation at the SR since it regulates SR-associated GAPDH activity [60]. Experiments designed to identify and delineate a role for CaMKIIβc in CDF and FDAR are ongoing. However, we hypothesize that CaMKIIβc may contribute to CDF and FDAR directly though phosphorylation events and indirectly by regulating glycolytic flux at the SR and/or the dyad space and that OGT plays a role in these activities. This is based on the following: 1) CaMKIIδ cannot account entirely for CDF [16], 2) CaMKIIβc autophosphorylation is also drastically reduced in OGTKO ventricles (Fig. 5C and E), 3) CaMKIIβc is likely O-GlcNAcylated (Fig. 6B) in basal conditions (i.e., in normoglycemia), 4) OGT and CaMKIIβc can be enriched from the same cellular location and both can apparently associate with calmodulin (Fig. 6A and [58]), 5) CDF is more sensitive to ATP levels when OGT is inhibited (Fig. 7), and 6) OGT activity is dictated, in part, by metabolite levels [21]. Experiments designed to investigate the relationship between OGT and CaMKIIβc and how they may impact cardiomyocyte Ca^{2+} handling are ongoing.

4.3. Comparison of the two models of reduced O-GlcNAcylation

In both the chronic genetic OGTKO model and the acute pharmacologic OSMI-1 model we observed a similar ~60% reduction in CDF-induced I_{Ca} potentiation following *OGT* ablation or OGT inhibition (Figs. 1A and B and 2A and B). There were however two major differences between the acute and chronic models of reduced O-GlcNAcylation although some differences between the models should not be surprising. That is, *OGT* is ablated in the OGTKO model, resulting in almost no OGT expression nor enzymatic activity chronically [27] while in the OSMI-1 model, enzymatic activity of OGT is only transiently inhibited. Thus, the genetic model abolishes enzymatic activity as well as any pleiotropic effects of *OGT* (i.e., structural interactions of OGT with other proteins, etc.). Additionally, we observed a number of remodeling events in the OGTKO including a down-regulation of Ca_v expression and a reduction in hemodynamic function that would likely impact neurohormonal regulation of the heart [27]. In this study, we show further examples of remodeling in the OGTKO model in the form of increased CaMKIIδ and calmodulin expression (Fig. 5A, B and E).

The first major functional difference between the two models was that the percent increase in $T_{0.37}$ (slowing of inactivation between P1 and P2 currents) observed during CDF was significantly reduced in the OGTKO model compared to TCre controls (Fig. 1D) while we observed no difference in the percent increase in $T_{0.37}$ during CDF between OSMI-1 and vehicle treated cardiomyocytes (Fig. 2D). Secondly, we observed a significant slowing of recovery from Ca_v inactivation in OSMI-1 treated cardiomyocytes (Fig. 3D), which is consistent with other studies investigating the impact of CaMKII inhibition on Ca_v recovery [5,11,43–45], but we observed an acceleration of recovery in OGTKO cardiomyocytes (Fig. 3A). The most likely explanation for these divergencies between models originates from their differences in intracellular Ca^{2+} levels following stimulation (systolic Ca^{2+}), with OGTKO cardiomyocytes demonstrating markedly reduced I_{Ca} and Ca^{2+} transient amplitude (Fig. 1E and [27] and OSMI-1 treated cardiomyocytes showing only marginal reductions in I_{Ca} (Fig. 2E) and no reduction in Ca^{2+} transient amplitude.

While most ascribe CDF to CaMKII activity (positive feedback), others have suggested that CDF is the consequence of reduced SR Ca^{2+} filling between repetitive stimulations that results in reduced Ca^{2+}-induced Ca^{2+} release and thus reduced CDI. Therefore, under this paradigm, I_{Ca} potentiation during facilitation is the result of slower Ca_v inactivation from the reduction in CDI (negative feedback) [50,51]. The data obtained using the OGTKO model where intracellular Ca^{2+} is

reduced (both I_{Ca} and Ca^{2+}-induced Ca^{2+} release) but CDF-induced I_{Ca} potentiation is also reduced could be construed as an argument against the negative feedback theory. However, it also suggests that CDF-induced I_{Ca} potentiation may be CaMKII-dependent while the slowing of inactivation is dependent on intracellular Ca^{2+} levels and thus the two are likely related but disparate processes. This is further supported by the fact that we observed reduced CDF-induced I_{Ca} potentiation yet no difference in Ca_v inactivation during facilitation in OSMI-1 treated cells, where I_{Ca} is only marginally reduced and Ca^{2+}-induced Ca^{2+} release is not affected. The reduction in OGTKO systolic intracellular Ca^{2+} likely also contributes to the inherently slower basal Ca_v inactivation rate that is not observed in OSMI-1 treated cardiomyocytes (Figs. 1C, 2C, and [27]).

Based on the experiments depicted in Fig. 3B, it is highly likely that the acceleration of Ca_v recovery from inactivation in OGTKO cardiomyocytes is also due to reduced intracellular systolic Ca^{2+} in that when control cells are used to model the reductions in OGTKO I_{Ca}, and presumably Ca^{2+}-induced Ca^{2+} release, by applying a smaller test potential (−10 mV), we observed a similar acceleration in Ca_v recovery compared to when we trigger larger I_{Ca} and thus Ca^{2+} release using a more depolarized test potential (10 mV; both test potentials occur along the linear portion of the conductance-voltage curve [27]). These data also suggest that intracellular Ca^{2+} plays a more prominent role in the rate of Ca_v recovery because, although CDF is reduced in OGTKO cardiomyocytes, likely due to inhibition of CaMKII, that is not enough to outweigh the impact of reduced systolic intracellular Ca^{2+} in the OGTKO on Ca_v recovery.

Taken together, while both have provided important insight into not only how OGT impacts CDF but also the underlying mechanisms responsible for CDF, the OGTKO and OSMI-1 models should only be considered complimentary and not equivalent models. In fact, one could argue that the OSMI-1 model is the superior model to investigate the direct effects of O-GlcNAcylation on the dynamic regulation of EC coupling and CaMKII activity while the OGTKO is better suited to uncover secondary and tertiary effects of OGT and O-GlcNAcylation on these processes.

4.4. Conclusions

In the present study, we shed new light on the scope to which O-GlcNAcylation (and/or OGT) contributes to cardiomyocyte EC coupling. OGT has long been thought to be a nucleocytoplasmic protein; however, our data indicate that OGT is also likely present at the SR and/or the dyad space where it contributes to the formation of a signaling complex that impacts cardiomyocyte Ca^{2+} handling. In contrast to work by others, this co-regulatory interaction between OGT and CaMKII occurs in the absence of hyperglycemia [28–31] indicating that the relationship between O-GlcNAcylation and CaMKII activity is more complicated than previously thought. Our data also indicate for the first time that OGT impacts the beat-to-beat regulation of Ca_v activity and cardiomyocyte EC coupling under basal conditions. These findings will enhance our current understanding of how disease processes that involve altered cellular signaling and metabolism, such as diabetes mellitus, hypertrophy and heart failure, may impact cardiomyocyte EC coupling though regulated and aberrant OGT and CaMKII activity.

Funding

This work was supported in part by grants from the National Science Foundation (Division of Molecular and Cellular Biosciences - 1856199 to A.R.E and E.S.B., Division of Integrative Organismal Systems - 1660926 to E.S.B.); and an American Heart Association Postdoctoral Fellowship (15POST25710010 to A.R.E).

Declaration of Competing Interest

None declared.

Appendix A. Supplementary data

Supplementary data to this article can be found online at https://doi.org/10.1016/j.yjmcc.2023.04.007.

References

[1] D.M. Bers, Cardiac excitation-contraction coupling, Nature 415 (6868) (2002) 198–205.
[2] A. Papa, J. Kushner, S.O. Marx, Adrenergic regulation of calcium channels in the heart, Annu. Rev. Physiol. 84 (2022) 285–306.
[3] D.M. Bers, S. Morotti, Ca(2+) current facilitation is CaMKII-dependent and has arrhythmogenic consequences, Front. Pharmacol. 5 (2014) 144.
[4] Z. Kubalová, Inactivation of L-type calcium channels in cardiomyocytes, Exp. Theoret. Approach. Gen. Physiol. Biophys. 22 (4) (2003) 441–454.
[5] E. Picht, J. DeSantiago, S. Huke, M.A. Kaetzel, J.R. Dedman, D.M. Bers, CaMKII inhibition targeted to the sarcoplasmic reticulum inhibits frequency-dependent acceleration of relaxation and Ca2+ current facilitation, J. Mol. Cell. Cardiol. 42 (1) (2007) 196–205.
[6] J. DeSantiago, L.S. Maier, D.M. Bers, Frequency-dependent acceleration of relaxation in the heart depends on CaMKII, but not phospholamban, J. Mol. Cell. Cardiol. 34 (8) (2002) 975–984.
[7] M.E. Anderson, A.P. Braun, H. Schulman, B.A. Premack, Multifunctional Ca2+/calmodulin-dependent protein kinase mediates Ca(2+)-induced enhancement of the L-type Ca2+ current in rabbit ventricular myocytes, Circ. Res. 75 (5) (1994) 854–861.
[8] R.P. Xiao, H. Cheng, W.J. Lederer, T. Suzuki, E.G. Lakatta, Dual regulation of Ca2+/calmodulin-dependent kinase II activity by membrane voltage and by calcium influx, Proc. Natl. Acad. Sci. U. S. A. 91 (20) (1994) 9659–9663.
[9] W. Yuan, D.M. Bers, Ca-dependent facilitation of cardiac Ca current is due to Ca-calmodulin-dependent protein kinase, Am. J. Phys. 267 (3 Pt 2) (1994) H982–H993.
[10] R.A. Bassani, A. Mattiazzi, D.M. Bers, CaMKII is responsible for activity-dependent acceleration of relaxation in rat ventricular myocytes, Am. J. Phys. 268 (2 Pt 2) (1995) H703–H712.
[11] J. Guo, H.J. Duff, Calmodulin kinase II accelerates L-type Ca2+ current recovery from inactivation and compensates for the direct inhibitory effect of [Ca2+]i in rat ventricular myocytes, J. Physiol. 574 (Pt 2) (2006) 509–518.
[12] A. Blaich, A. Welling, S. Fischer, J.W. Wegener, K. Köstner, F. Hofmann, S. Moosmang, Facilitation of murine cardiac L-type Ca(v)1.2 channel is modulated by calmodulin kinase II-dependent phosphorylation of S1512 and S1570, Proc. Natl. Acad. Sci. USA 107 (22) (2010) 10285–10289.
[13] T.S. Lee, R. Karl, S. Moosmang, P. Lenhardt, N. Klugbauer, F. Hofmann, T. Kleppisch, A. Welling, Calmodulin kinase II is involved in voltage-dependent facilitation of the L-type Cav1.2 calcium channel: identification of the phosphorylation sites, J. Biol. Chem. 281 (35) (2006) 25560–25567.
[14] C.F. Edman, H. Schulman, Identification and characterization of delta B-CaM kinase and delta C-CaM kinase from rat heart, two new multifunctional Ca2+/calmodulin-dependent protein kinase isoforms, Biochim. Biophys. Acta 1221 (1) (1994) 89–101.
[15] T. Tobimatsu, H. Fujisawa, Tissue-specific expression of four types of rat calmodulin-dependent protein kinase II mRNAs, J. Biol. Chem. 264 (30) (1989) 17907–17912.
[16] L. Xu, D. Lai, J. Cheng, H.J. Lim, T. Keskanokwong, J. Backs, E.N. Olson, Y. Wang, Alterations of L-type calcium current and cardiac function in CaMKII{delta} knockout mice, Circ. Res. 107 (3) (2010) 398–407.
[17] M.Y. Mollova, H.A. Katus, J. Backs, Regulation of CaMKII signaling in cardiovascular disease, Front. Pharmacol. 6 (2015) 178.
[18] J.R. Erickson, Mechanisms of CaMKII activation in the heart, Front. Pharmacol. 5 (2014) 59.
[19] M. Simon, C.Y. Ko, R.T. Rebbeck, S. Baidar, R.L. Cornea, D.M. Bers, CaMKIIδ post-translational modifications increase affinity for calmodulin inside cardiac ventricular myocytes, J. Mol. Cell. Cardiol. 161 (2021) 53–61.
[20] G.W. Hart, C. Slawson, G. Ramirez-Correa, O. Lagerlof, Cross talk between O-GlcNAcylation and phosphorylation: roles in signaling, transcription, and chronic disease, Annu. Rev. Biochem. 80 (2011) 825–858.
[21] M.R. Bond, J.A. Hanover, A little sugar goes a long way: the cell biology of O-GlcNAc, J. Cell Biol. 208 (7) (2015) 869–880.
[22] Q. Ong, W. Han, X. Yang, O-GlcNAc as an integrator of signaling pathways, Front. Endocrinol. 9 (2018) 599.
[23] S. Ducheix, J. Magré, B. Cariou, X. Prieur, Chronic O-GlcNAcylation and diabetic cardiomyopathy: the bitterness of glucose, Front. Endocrinol. 9 (2018) 642.
[24] J.N. Wright, H.E. Collins, A.R. Wende, J.C. Chatham, O-GlcNAcylation and cardiovascular disease, Biochem. Soc. Trans. 45 (2) (2017) 545–553.

[25] D.H. Tran, Z.V. Wang, Glucose metabolism in cardiac hypertrophy and heart failure, J. Am. Heart Assoc. 8 (12) (2019), e012673.
[26] H.E. Collins, J.C. Chatham, Regulation of cardiac O-GlcNAcylation: more than just nutrient availability, Biochim. Biophys. Acta. Mol. Basis Disease 1866 (5) (2020), 165712.
[27] A.R. Ednie, E.S. Bennett, Intracellular O-linked glycosylation directly regulates cardiomyocyte L-type Ca(2+) channel activity and excitation-contraction coupling, Basic Res. Cardiol. 115 (6) (2020) 59.
[28] B. Hegyi, A. Fasoli, C.Y. Ko, B.W. Van, C.C. Alim, E.Y. Shen, M.M. Ciccozzi, S. Tapa, C.M. Ripplinger, J.R. Erickson, J. Bossuyt, D.M. Bers, CaMKII serine 280 O-GlcNAcylation links diabetic hyperglycemia to proarrhythmia, Circ. Res. 129 (1) (2021) 98–113.
[29] J.R. Erickson, L. Pereira, L. Wang, G. Han, A. Ferguson, K. Dao, R.J. Copeland, F. Despa, G.W. Hart, C.M. Ripplinger, D.M. Bers, Diabetic hyperglycaemia activates CaMKII and arrhythmias by O-linked glycosylation, Nature 502 (7471) (2013) 372–376.
[30] B. Hegyi, J.M. Borst, L.R.J. Bailey, E.Y. Shen, A.J. Lucena, M.F. Navedo, J. Bossuyt, D.M. Bers, Hyperglycemia regulates cardiac K(+) channels via O-GlcNAc-CaMKII and NOX2-ROS-PKC pathways, Basic Res. Cardiol. 115 (6) (2020) 71.
[31] S. Lu, Z. Liao, X. Lu, D.M. Katschinski, M. Mercola, J. Chen, J. Heller Brown, J. D. Molkentin, J. Bossuyt, D.M. Bers, Hyperglycemia acutely increases cytosolic reactive oxygen species via O-linked GlcNAcylation and CaMKII activation in mouse ventricular myocytes, Circ. Res. 126 (10) (2020) e80–e96.
[32] L.J. Watson, H.T. Facundo, G.A. Ngoh, M. Ameen, R.E. Brainard, K.M. Lemma, B. W. Long, S.D. Prabhu, Y.T. Xuan, S.P. Jones, O-linked β-N-acetylglucosamine transferase is indispensable in the failing heart, Proc. Natl. Acad. Sci. U. S. A. 107 (41) (2010) 17797–17802.
[33] J.B. Berletch, F. Yang, C.M. Disteche, Escape from X inactivation in mice and humans, Genome Biol. 11 (6) (2010) 213.
[34] K. Bersell, S. Choudhury, M. Mollova, B.D. Polizzotti, B. Ganapathy, S. Walsh, B. Wadugu, S. Arab, B. Kühn, Moderate and high amounts of tamoxifen in αMHC-MerCreMer mice induce a DNA damage response, leading to heart failure and death, Dis. Model. Mech. 6 (6) (2013) 1459–1469.
[35] K.B. Andersson, L.H. Winer, H.K. Mørk, J.D. Molkentin, F. Jaisser, Tamoxifen administration routes and dosage for inducible Cre-mediated gene disruption in mouse hearts, Transgenic Res. 19 (4) (2010) 715–725.
[36] A.R. Ednie, A.R. Parrish, M.J. Sonner, E.S. Bennett, Reduced hybrid/complex N-glycosylation disrupts cardiac electrical signaling and calcium handling in a model of dilated cardiomyopathy, J. Mol. Cell. Cardiol. 132 (2019) 13–23.
[37] A.R. Ednie, W. Deng, K.P. Yip, E.S. Bennett, Reduced myocyte complex N-glycosylation causes dilated cardiomyopathy, FASEB J. Off. Publ. Federat. Am. Soc. Exp. Biol. 33 (1) (2019) 1248–1261.
[38] A.R. Ednie, E.S. Bennett, Reduced sialylation impacts ventricular repolarization by modulating specific K+ channel isoforms distinctly, J. Biol. Chem. 290 (5) (2015) 2769–2783.
[39] R.N. Harris, J.H. Doroshow, Effect of doxorubicin-enhanced hydrogen peroxide and hydroxyl radical formation on calcium sequestration by cardiac sarcoplasmic reticulum, Biochem. Biophys. Res. Commun. 130 (2) (1985) 739–745.
[40] W. Fuller, P. Eaton, R.A. Medina, J. Bell, M.J. Shattock, Differential centrifugation separates cardiac sarcolemmal and endosomal membranes from Langendorff-perfused rat hearts, Anal. Biochem. 293 (2) (2001) 216–223.
[41] S. Bolte, F.P. Cordelières, A guided tour into subcellular colocalization analysis in light microscopy, J. Microsc. 224 (Pt 3) (2006) 213–232.
[42] R.F. Ortiz-Meoz, J. Jiang, M.B. Lazarus, M. Orman, J. Janetzko, C. Fan, D. Y. Duveau, Z.W. Tan, C.J. Thomas, S. Walker, A small molecule that inhibits OGT activity in cells, ACS Chem. Biol. 10 (6) (2015) 1392–1397.
[43] E. Martinez-Hernandez, L.A. Blatter, G. Kanaporis, L-type Ca(2+) channel recovery from inactivation in rabbit atrial myocytes, Physiol. Rep. 10 (5) (2022), e15222.
[44] T.M. Vinogradova, Y.Y. Zhou, K.Y. Bogdanov, D. Yang, M. Kuschel, H. Cheng, R. P. Xiao, Sinoatrial node pacemaker activity requires Ca(2+)/calmodulin-dependent protein kinase II activation, Circ. Res. 87 (9) (2000) 760–767.
[45] L. Li, H. Satoh, K.S. Ginsburg, D.M. Bers, The effect of Ca(2+)-calmodulin-dependent protein kinase II on cardiac excitation-contraction coupling in ferret ventricular myocytes, J. Physiol. 501 (Pt 1) (1997) 17–31.
[46] L.V. Hryshko, D.M. Bers, Ca current facilitation during postrest recovery depends on Ca entry, Am. J. Phys. 259 (3 Pt 2) (1990) H951–H961.
[47] J.W. Bassani, W. Yuan, D.M. Bers, Fractional SR Ca release is regulated by trigger Ca and SR Ca content in cardiac myocytes, Am. J. Phys. 268 (5 Pt 1) (1995) C1313–C1319.
[48] G.N. Tseng, Calcium current restitution in mammalian ventricular myocytes is modulated by intracellular calcium, Circ. Res. 63 (2) (1988) 468–482.
[49] D. Fedida, D. Noble, A.J. Spindler, Use-dependent reduction and facilitation of Ca2+ current in guinea-pig myocytes, J. Physiol. 405 (1988) 439–460.
[50] C. Delgado, A. Artiles, A.M. Gómez, G. Vassort, Frequency-dependent increase in cardiac Ca2+ current is due to reduced Ca2+ release by the sarcoplasmic reticulum, J. Mol. Cell. Cardiol. 31 (10) (1999) 1783–1793.
[51] J. Guo, H.J. Duff, Inactivation of ICa-L is the major determinant of use-dependent facilitation in rat cardiomyocytes, J. Physiol. 547 (Pt 3) (2003) 797–805.
[52] T.J. Schoenmakers, G.J. Visser, G. Flik, A.P., Theuvenet, CHELATOR: an improved method for computing metal ion concentrations in physiological solutions, BioTechniques 12 (6) (1992) 870–874, 876–9.
[53] S.E. Bates, A.M. Gurney, Use-dependent facilitation and depression of L-type Ca2+ current in guinea-pig ventricular myocytes: modulation by Ca2+ and isoprenaline, Cardiovasc. Res. 44 (2) (1999) 381–389.
[54] Y. Wu, L.B. MacMillan, R.B. McNeill, R.J. Colbran, M.E. Anderson, CaM kinase augments cardiac L-type Ca2+ current: a cellular mechanism for long Q-T arrhythmias, Am. J. Phys. 276 (6) (1999) H2168–H2178.
[55] A.C. Zygmunt, J. Maylie, Stimulation-dependent facilitation of the high threshold calcium current in guinea-pig ventricular myocytes, J. Physiol. 428 (1990) 653–671.
[56] A. Hudmon, H. Schulman, Structure-function of the multifunctional Ca2+/calmodulin-dependent protein kinase II, Biochem. J. 364 (Pt 3) (2002) 593–611.
[57] K.U. Bayer, K. Harbers, H. Schulman, alphaKAP is an anchoring protein for a novel CaM kinase II isoform in skeletal muscle, EMBO J. 17 (19) (1998) 5598–5605.
[58] P. Singh, M. Salih, B.S. Tuana, Alpha-kinase anchoring protein alphaKAP interacts with SERCA2A to spatially position Ca2+/calmodulin-dependent protein kinase II and modulate phospholamban phosphorylation, J. Biol. Chem. 284 (41) (2009) 28212–28221.
[59] P. Singh, J.J. Leddy, G.J. Chatzis, M. Salih, B.S. Tuana, Alternative splicing generates a CaM kinase IIbeta isoform in myocardium that targets the sarcoplasmic reticulum through a putative alphaKAP and regulates GAPDH, Mol. Cell. Biochem. 270 (1–2) (2005) 215–221.
[60] P. Singh, M. Salih, J.J. Leddy, B.S. Tuana, The muscle-specific calmodulin-dependent protein kinase assembles with the glycolytic enzyme complex at the sarcoplasmic reticulum and modulates the activity of glyceraldehyde-3-phosphate dehydrogenase in a Ca2+/calmodulin-dependent manner, J. Biol. Chem. 279 (34) (2004) 35176–35182.
[61] G. Liu, A. Papa, A.N. Katchman, S.I. Zakharov, D. Roybal, J.A. Hennessey, J. Kushner, L. Yang, B.X. Chen, A. Kushnir, K. Dangas, S.P. Gygi, G.S. Pitt, H. M. Colecraft, M. Ben-Johny, M. Kalocsay, S.O. Marx, Mechanism of adrenergic Ca (V)1.2 stimulation revealed by proximity proteomics, Nature 577 (7792) (2020) 695–700.
[62] K.Y. Xu, J.L. Zweier, L.C. Becker, Functional coupling between glycolysis and sarcoplasmic reticulum Ca2+ transport, Circ. Res. 77 (1) (1995) 88–97.
[63] K.Y. Xu, L.C. Becker, Ultrastructural localization of glycolytic enzymes on sarcoplasmic reticulum vesticles, J. Histochem. Cytochem. Off. J. Histochem. Soc. 46 (4) (1998) 419–427.
[64] M. Hussain, G.A. Drago, J. Colyer, C.H. Orchard, Rate-dependent abbreviation of Ca2+ transient in rat heart is independent of phospholamban phosphorylation, Am. J. Phys. 273 (2 Pt 2) (1997) H695–H706.
[65] S.J. Coultrap, I. Buard, J.R. Kulbe, M.L. Dell'Acqua, K.U. Bayer, CaMKII autonomy is substrate-dependent and further stimulated by Ca2+/calmodulin, J. Biol. Chem. 285 (23) (2010) 17930–17937.
[66] S. Strack, M.A. Barban, B.E. Wadzinski, R.J. Colbran, Differential inactivation of postsynaptic density-associated and soluble Ca2+/calmodulin-dependent protein kinase II by protein phosphatases 1 and 2A, J. Neurochem. 68 (5) (1997) 2119–2128.
[67] R.J. Colbran, Protein phosphatases and calcium/calmodulin-dependent protein kinase II-dependent synaptic plasticity, J. Neurosci. 24 (39) (2004) 8404–8409.
[68] T. Toyofuku, K. Curotto Kurzydlowski, N. Narayanan, D.H. MacLennan, Identification of Ser38 as the site in cardiac sarcoplasmic reticulum Ca(2+)-ATPase that is phosphorylated by Ca2+/calmodulin-dependent protein kinase, J. Biol. Chem. 269 (42) (1994) 26492–26496.
[69] A. Xu, C. Hawkins, N. Narayanan, Phosphorylation and activation of the Ca(2+)-pumping ATPase of cardiac sarcoplasmic reticulum by Ca2+/calmodulin-dependent protein kinase, J. Biol. Chem. 268 (12) (1993) 8394–8397.
[70] A. Odermatt, K. Kurzydlowski, D.H. MacLennan, The vmax of the Ca2+-ATPase of cardiac sarcoplasmic reticulum (SERCA2a) is not altered by Ca2+/calmodulin-dependent phosphorylation or by interaction with phospholamban, J. Biol. Chem. 271 (24) (1996) 14206–14213.
[71] L.G. Reddy, L.R. Jones, R.C. Pace, D.L. Stokes, Purified, reconstituted cardiac Ca2+-ATPase is regulated by phospholamban but not by direct phosphorylation with Ca2+/calmodulin-dependent protein kinase, J. Biol. Chem. 271 (25) (1996) 14964–14970.